Comparative Biochemistry and Physiology, Part A 164 (2013) 327–332

Contents lists available at SciVerse ScienceDirect

Comparative Biochemistry and Physiology, Part A

journal homepage: www.elsevier.com/locate/cbpa

Neuroendocrine responses of a crustacean host to viral infection: Effects of infection of white spot syndrome virus on the expression and release of crustacean hyperglycemic hormone in the crayfish *Procambarus clarkii*

Ling-Jiun Lin [a], Yan-Jhou Chen [a], Yun-Shiang Chang [b], Chi-Ying Lee [c,*]

[a] Department of Biology, National Changhua University of Education, Changhua 50058, Taiwan
[b] Department of Molecular Biotechnology, Da-Yeh University, Changhua 51591, Taiwan
[c] Graduate Institute of Biotechnology, National Changhua University of Education, Changhua 50058, Taiwan

ARTICLE INFO

Article history:
Received 9 September 2012
Received in revised form 13 November 2012
Accepted 14 November 2012
Available online 19 November 2012

Keywords:
White spot syndrome virus
Crustacean hyperglycemic hormone
Carbohydrate metabolism
Glycolysis

ABSTRACT

The objectives of the present study were to characterize the changes in crustacean hyperglycemic hormone (CHH) transcript and peptide levels in response to infection of white spot syndrome virus (WSSV) in a crustacean, *Procambarus clarkii*. After viral challenge, significant increase in virus load began at 24 h post injection (hpi) and the increase was much more substantial at 48 and 72 hpi. The hemolymph CHH levels rapidly increased after viral challenge; the increase started as early as 3 hpi and lasted for at least 2 d after the challenge. In contrast, the hemolymph glucose levels did not significantly changed over a 2 d period in the WSSV-infected animals. The CHH transcript and peptide levels in tissues were also determined. The CHH transcript levels in the eyestalk ganglia (the major site of CHH synthesis) of the virus-infected animals did not significantly change over a 2 d period and those in 2 extra-eyestalk tissues (the thoracic ganglia and cerebral ganglia) significantly increased at 24 and 48 hpi. The CHH peptide levels in the eyestalk ganglia of the virus-infected animals significantly decreased at 24 and 48 hpi and those in the thoracic ganglia and cerebral ganglia remained unchanged over a 2 d period. These data demonstrated a WSSV-induced increase in the release of CHH into hemolymph that is rapid in onset and lasting in duration. Changes in the CHH transcript and peptide levels implied that the WSSV-induced increase in hemolymph CHH levels primarily resulted from an enhanced release from the eyestalk ganglia, but the contribution of the 2 extra-eyestalk tissues to hemolymph pool of CHH increased as viral infection progressed. The combined patterns of change in the hemolymph glucose and CHH levels further suggest that the virus-enhanced CHH release would lead to higher glycolytic activity and elevated glucose mobilization presumably favorable for viral replication.

1. Introduction

White spot disease (WSD) is a highly contagious and lethal viral disease of penaeid shrimps caused by an infection of white spot syndrome virus (WSSV), which is an enveloped, rod-shaped virus containing a double-stranded DNA genome. WSSV has a wide range of potential hosts including more than 90 species of arthropods. It is highly virulent and leads to extremely high mortality rates within days in the case of cultured shrimp populations. Thus, it poses serious threats in particular to shrimp aquaculture, causing tremendous loss to the global farming industry since the first documented disease outbreak in the early 1990 (Sánchez-Paz, 2010).

Although therapeutic measures for effective control of WSSV infection are currently unavailable, much has been learned about WSSV regarding its morphology, ultrastructure, genome, gene expression pattern, and mode of transmission, etc. (see Escobedo-Bonilla et al., 2008; Leu et al., 2009; Sánchez-Paz, 2010). Despite the host–virus interaction has been one of the recent focuses in understanding WSSV pathogenesis (Jiravanichpaisal et al., 2006; Leu et al., 2007, 2012; Wang et al., 2007; Rodríguez et al., 2012), the responses of the host endocrine system to WSSV infection have yet to be characterized.

Crustacean hyperglycemic hormone (CHH) is a polypeptide hormone originally identified in an important crustacean neuroendocrine tissue, the X-organ/sinus gland complex, located within the eyestalks (see Keller, 1992; Soyez, 1997); more recent studies have firmly established that CHH is also expressed in several other extra-eyestalk neuroendocrine tissues (see Webster et al., 2012). CHH belongs to a family of polypeptide hormones, the CHH family (Kegel et al., 1991; Soyez, 1997), which also includes molt-inhibiting hormone (MIH), vitellogenesis-inhibiting hormone (VIH), and mandibular organ-inhibiting hormone (MOIH), and insect ion transport peptide (ITP) (Chen et al., 2005). Recent studies have expanded the existence of the CHH family peptides beyond arthropods to ecdysozoans (Christie, 2008; Montagné et al., 2010).

* Corresponding author at: Graduate Institute of Biotechnology, National Changhua University of Education, 1 Jin Der Road, Changhua 50058, Taiwan. Tel.: +886 4 724 7756; fax: +886 4 721 1156.
E-mail address: bicylee@cc.ncue.edu.tw (C.-Y. Lee).

1095-6433/$ – see front matter © 2012 Elsevier Inc. All rights reserved.
http://dx.doi.org/10.1016/j.cbpa.2012.11.009

Functionally, CHH plays regulatory roles in the main pathways of carbohydrate metabolism (see Santos and Keller 1993) and is considered a stress hormone that is critically involved in eliciting stress-induced hyperglycemia (Webster, 1996; Chang et al., 1998, 1999; Zou et al., 2003; Lorenzon et al., 2004; Webster et al., 2012). In light of the observations that viral infection is usually associated with changes in carbohydrate metabolism in mammalian hosts (see Yu et al., 2011; Noch and Khalili, 2012), it was reasoned that CHH would probably constitute an important part of the endocrine responses to viral infection in crustaceans and the responses might bear significant implication for understanding viral pathogenesis and identifying potential targets for therapeutic intervention. As a first effort in characterizing the endocrine responses to WSSV infection, the aims of the present study were to determine the effects of WSSV infection on a crustacean host *Procambarus clarkii*, specifically the effects on CHH expression in various neuroendocrine tissues and its release into the circulation.

2. Materials and methods

2.1. Animals

Animals (*P. clarkii*) were purchased from local fisherman and maintained in the laboratory as previously described (Zou et al., 2003). Animals used in the present study were intermolt adults that had been determined to be WSSV-free using a polymerase chain reaction (PCR)-based diagnostic kit IQ2000™ (GeneReach Biotechnology Corp.) according to the manufacturer's protocol.

2.2. Virus and viral challenge

The viral preparations (WSSV-TW strain, GenBank accession no. AF440570) were kindly provided by the Core Facilities for Shrimp Functional Genomics (SFGC) (http://shrimpwssv.lifescience.ntu.edu.tw). The WSSV-TW strain (Chang et al. 2008) originates from a batch of WSSV-infected *Penaeus monodon* collected in Taiwan in 1994 (Wang et al. 1995; Lo et al. 1999). The preparations were stored at −80 °C and before use diluted with sterile 0.01 M phosphate-buffered saline (PBS) and filtered through a 0.45 μm filter.

Before experimental procedures, animals were deprived of food for 1 d. They were then each injected with 100 μl of diluted viral solution (2×10^6 particles/animal) or 0.01 M PBS (as vehicle controls) using an insulin syringe coupled to a 29-gauge needle (Terumo Medical Corp., Elkton, MD). Tissues and hemolymph samples (see below) were collected from animals before injection (taken as time zero) and at designated time points thereafter for subsequent analyses.

2.3. Absolute quantification of virus load by real-time polymerase chain reaction (PCR)

A real time PCR assay for viral ICP11 gene (GenBank accession numbers HM778020) (Chang et al., 2011) was employed for absolute quantification of the WSSV copy number in the experimental animals (see Section 2.2.). The genomic DNA was extracted from the pleopods of the animals using the reagents supplied with the IQ2000™ kit and the extracted samples were amplified using a commercially available kit (LightCycler FastStart DNA Master SYBR Green I, Roche) in a 10-μl reaction according to the manufacturer's protocol. Reactions were performed under the following conditions: an initial denaturation (10 min, 95 °C), 40 cycles of denaturation (10 s, 95 °C), annealing (7 s, 55 °C), and extension (13 s, 72 °C). Primers used were ICP11-F-real and ICP11-R-real (see Table 1). Standard curves were constructed by plotting the copy number of ICP11 gene (pGEM/ICP11, Chang et al., 2011) vs. the threshold cycle (C_t) value of the PCR reaction (see Fig. 1).

Table 1
Sequences of primers used in the present study for the real-time quantitative polymerase chain reactions.

Primer	Sequence (5′ to 3′)	Accession number
ICP11-F-real	AGGCAGTCAGGAAGAGTGATCTAGA	HM778020
ICP11-R-real	AATTCTTCGATGCCTCCATTGA	
CHHe2F	AACCTCTCAGCTTCCTCTCCCAAG	AB027291
SG-R-400-427	CATAGCAGTTTTGTCTGCAGGTGGTGGC	
GAPDH-F-209	TCATGGTGTGTTCAAGGGT	AB094145
GAPDH-R-361	AGAGGCTTTCTCAATAGTGG	

2.4. Relative quantification of the levels of CHH transcript by real-time PCR

The levels of CHH transcript in tissues were measured by a real-time PCR assay. Tissues (eyestalk ganglia, thoracic ganglia, and cerebral ganglia) dissected from experimental animals (see Section 2.2.) were processed for total RNA extraction and reverse transcription according to described protocols (Tsai et al., 2008).

For real-time PCR, cDNA templates were amplified in a 10-μl reaction using the same LightCycler reagents mentioned above. Reactions were performed under the following conditions: an initial denaturation (10 min, 95 °C), 50 cycles of denaturation (10 s, 95 °C), annealing (7 s, 60 °C), and extension (14 s, 72 °C); the rate of temperature change was 20 °C/s. The primers used were CHHe2F and SG-R-400-427 for PCR amplification of *CHH* (see Table 1). The forward primer (CHHe2F) covers a sequence encoding the 21st to 28th residues of the CHH-precursor related peptide, a stretch that is common in sequence to both the CHH and CHH-like (CHH-L) precursors (Wu et al., 2012a). The specificity of the PCR for CHH relies on the backward primer (SG-R-400-427, see Table 1), which covers a continuous sequence spanning from exon II to exon IV of CHH transcript (that is composed of exons I, II, and IV). Thus, amplification using SG-R-400-427 together with the forward primer would be expected to specifically amplify the transcript encoding CHH, but not the CHH-L transcript (that is composed of exons I, II, III and IV) (Wu et al., 2012a). Sequence analysis of the sole PCR product amplified using the primer pair confirmed that the product encodes CHH, not CHH-L (data not shown). Primers used for amplification of the reference gene glyceraldehyde-3 phosphate dehydrogenase (*GAPDH*) were GAPDH-F-209 and GAPDH-R-361 (see Table 1). Glyceraldehyde-3 phosphate dehydrogenase gene was selected as the reference gene on the ground that preliminary tests indicated that for each examined tissue the threshold cycle value for its

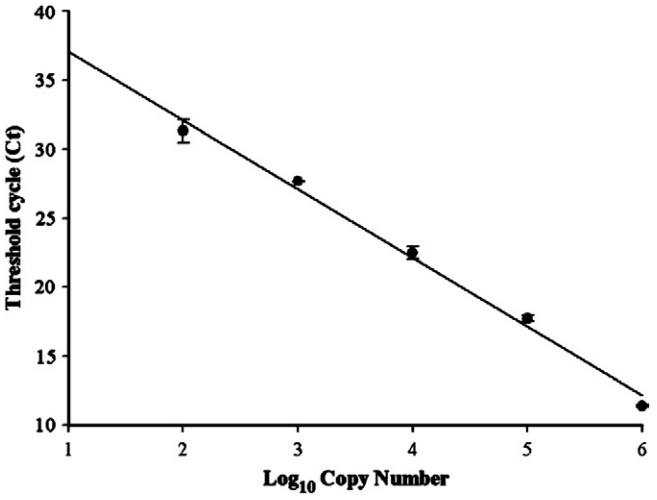

Fig. 1. A typical standard curve for quantification of the viral ICP11 gene by a real-time PCR. A series of diluted plasmid DNA samples (pGEM/ICP11) with a range of 1×10^2–1×10^6 copies of ICP11 was real-time PCR-amplified. The threshold cycle (C_t) of each reaction was plotted against the log-transformed copy number. (n = 5 for each data point).

amplification was not statistically different among pre-injected, vehicle control, and virus-challenged animals (data not shown).

Amplification efficiency and specificity were validated according to previously described methods (Chen et al., 2007). The calculated amplification efficiency was always greater than 90% for the 2 amplicons (*CHH* and *GAPDH*). To ensure amplification specificity, melting curve analysis was performed from 65 °C to 94 °C at the rate of 0.1 °C/s after PCR reaction. The results of melting curve analyses of each PCR reaction showed a single peak indicating the amplification specificity (data not shown).

The comparative threshold cycle method (Livak and Schmittgen, 2001) was used to determine the transcript levels. Briefly, transcript levels of CHH were normalized to those of GAPDH, and the normalized levels at each time points after injection were expressed relative to the zero time levels (arbitrarily designated as the calibrator) according to previously described equations (Chen et al., 2007).

2.5. Sandwich enzyme-linked immunosorbent assay (ELISA) and glucose assay

Tissues (eyestalk ganglia, thoracic ganglia, and cerebral ganglia) dissected from experimental animals (see Section 2.2.) were processed according to Wu et al. (2012b) for ELISA quantification of CHH. Another set of experimental animals were used for collecting and processing of hemolymph samples (Yeh et al., 2006) for quantification of hemolymph CHH and glucose levels. The protocols and reagents for CHH ELISA and glucose assay have been described in Wu et al. (2012a,b).

2.6. Statistical analysis

Effects of the viral challenge on the measured parameters were analyzed by one-way analysis of variance followed by Tukey's HSD test or by Student's *t*-test using computer software (SPSS Manager, SPSS Inc.). The data are reported as the mean ± standard deviation.

3. Results

Absolute quantification of the viral copy number by a real-time PCR assay revealed that a significant increase in virus load in the WSSV-infected animals occurred at 24 h post injection (hpi), and the increase were much more substantial at 48 and 72 hpi, exceeding more than 1000 copies/ng of total DNA (Fig. 2).

The hemolymph CHH levels were quantified by a CHH-specific sandwich ELISA. In the WSSV-infected animals, the levels significantly increased as early as 3 hpi, peaked at 12 hpi, and remained significantly elevated at 48 hpi when compared to the levels at 0 hpi (Fig. 3). There was no significant change in the hemolymph CHH levels over time in the PBS-treated animals (Fig. 3). The glucose levels in the WSSV-infected animals, similar to those in the PBS-treated animals, did not statistically change over time after injection (Fig. 4).

Transcript levels in the tissues were quantified by a relative real-time PCR. In the WSSV-infected animals, the CHH transcript levels were significantly increased in the thoracic ganglia and cerebral ganglia at 24 and 48 hpi when compared to those at 0 hpi (Fig. 5B, C), whereas the levels did not significantly change in the eyestalk ganglia at any time point measured (Fig. 5A). There was no significant change in CHH transcript levels in any of the tested tissues of the PBS-treated animals (Fig. 5A, B, C).

The CHH peptide levels measured by the ELISA indicated that they significantly decreased in the eyestalk ganglia of the WSSV-infected animals at 24 and 48 hpi when compared to those at 0 hpi (Fig. 6A), whereas the levels did not significantly changed in the thoracic ganglia or cerebral ganglia at any time point measured (Fig. 6B, C). There was no significant change in CHH peptide levels in any of the tested tissues of the PBS-treated animals (Fig. 6A, B, C).

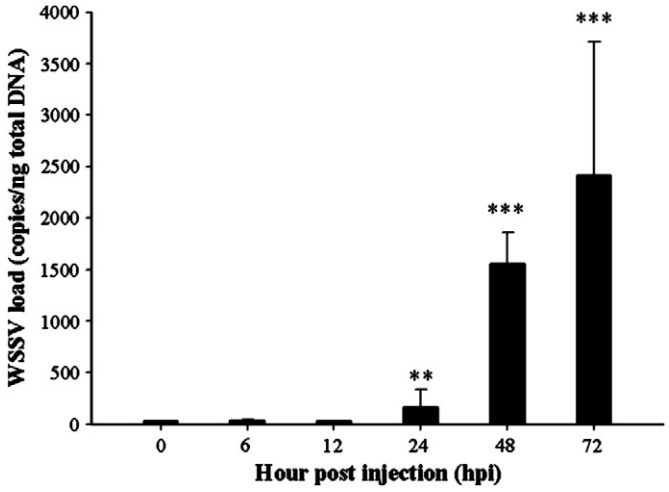

Fig. 2. Temporal profile of changes in the virus load in the white spot syndrome virus-infected crayfish. Animals were challenged with an injection of 0.01 M PBS containing 2×10^6 viral particles. The genomic DNA extracted from the pleopods harvested from the animals before and at designated time points after injection was analyzed by a real-time polymerase chain reaction for quantification of the viral ICP11 gene (accession number HM778020). **, *** represent significant differences from the zero time values at the levels of 0.01 and 0.005, respectively (n = 5 for each time point).

4. Discussion

Based on decades of research, it is well established that stressors of various natures (thermal stress, hypoxia, organic and inorganic pollutants, bacterial infection, etc.) elicit the CHH-mediated hyperglycemia (see Chang et al. 1999; Webster et al., 2012). The present report represents the first study investigating the effects of white spot syndrome virus (WSSV) on the endocrine system of a crustacean host. A rapid and lasting (for at least 2 d) increase in hemolymph CHH levels was observed in the WSSV-infected animals, reflecting an enhanced release from tissues. Onset of the response of WSSV-induced CHH release to viral challenge commenced as early as 3 hpi when viral load has not yet significantly increased. Sustained duration of CHH release such as that elicited by WSSV challenge reported in the present study has not been previously documented, and it emphasizes that the capacity of

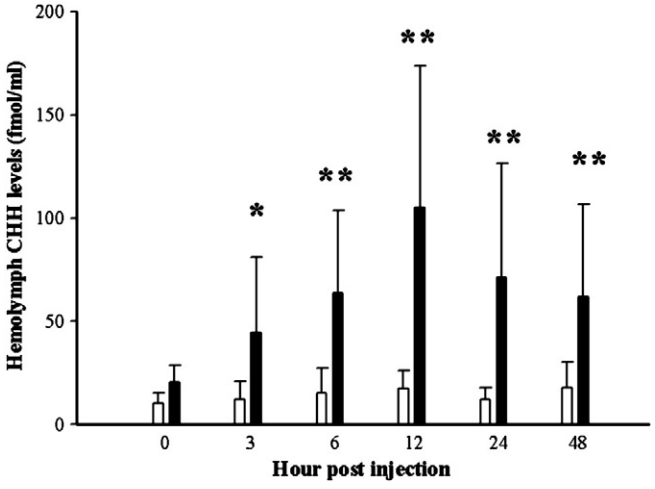

Fig. 3. Temporal profile of changes in the hemolymph levels of CHH in white spot syndrome virus-infected and vehicle-treated crayfish. Animals were challenged with an injection of 0.01 M PBS (white bar) or PBS containing 2×10^6 viral particles (black bar). Hemolymph withdrawn from the animals before and at designated time points after injection was quantified by ELISA for CHH levels. *, ** represent significant differences from the zero time values at the levels of 0.05 and 0.01, respectively (n = 8 for each time point).

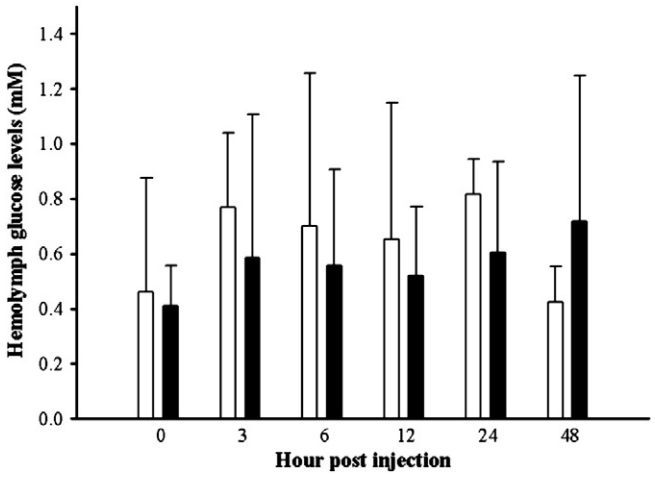

Fig. 4. Temporal profile of changes in the hemolymph glucose levels in white spot syndrome virus-infected and vehicle-treated crayfish. Animals were challenged with an injection of 0.01 M PBS (white bar) or PBS containing 2×10^6 viral particles (black bar). Hemolymph withdrawn from the animals before and at designated time points after injection was analyzed for quantification of glucose levels. n = 8 for each time point.

CHH release under stressful environment could last for days, although tissue reserves tend to deplete in the major site of CHH synthesis — the eyestalk ganglia (see below).

The profiles of changes in CHH transcript and CHH peptide levels in tissues after viral challenge are different between, the eyestalk ganglia, on the one hand, and the thoracic ganglia and cerebral ganglia, on the other. CHH gene expression, as estimated by its transcript levels, in the eyestalk ganglia remained essentially unchanged over time in the virus-challenged animals. Coupled to an enhanced release of CHH into hemolymph as mentioned above, this would explain the observation that CHH peptide levels in the eyestalk ganglia dramatically decreased to about one fifth of the pre-challenge levels at 48 hpi. In contrast, CHH gene expression in the thoracic ganglia and cerebral ganglia was up-regulated while CHH peptide levels in these tissues were not significantly changed after viral challenge. Although the relative contribution of the eyestalk ganglia and the 2 extra-eyestalk tissues to the hemolymph CHH could not be directly inferred from the data, it appears that as the viral replication progresses in the hosts the importance of the thoracic ganglia and cerebral ganglia as the sites of CHH synthesis and release is increasing. The physiological and pathophysiological significances of the thoracic ganglia and cerebral ganglia being activated while the eyestalk ganglia becoming rather quiescent after the viral challenge are not presently clear. It could be that the eyestalk ganglia were getting disrupted in terms of its secretory capacity and that the 2 extra-eyestalk tissues were mounting a compensatory response for CHH biosynthesis and secretion.

An intriguing profile of changes in the hemolymph glucose levels after viral challenge was observed: despite the hemolymph CHH levels rapidly increased as mentioned above, the glucose levels did not statistically change over time after viral challenge. This is in contrast with previously reported data where the stress-induced release of CHH into hemolymph almost invariably led to hyperglycemic responses (Webster 1996; Chang et al. 1998; Zou et al., 2003; Lorenzon et al. 2004; Morris et al., 2010). The apparent absence of a CHH-evoked hyperglycemia under viral challenge could be resulted from a virally enhanced glycolytic flux, glucose uptake, or both, by the host cells, which would effectively counteract the CHH-evoked hyperglycemic response. Virus-induced alterations of glucose uptake, glucose metabolism, or both, favorable for viral replication and disease progression have been reported in mammalian hosts (see e.g., Abrantes et al., 2012; Noch and Khalili, 2012; Silva da Costa et al., 2012), and recently in a crustacean (Chen et al., 2011). Interestingly enough, a recent report showed that a putative glucose transporter (Glut1) expressed on the surface of the host cells might assist WSSV entry by serving as a virus-binding receptor (Huang et al., 2012); whether the functional

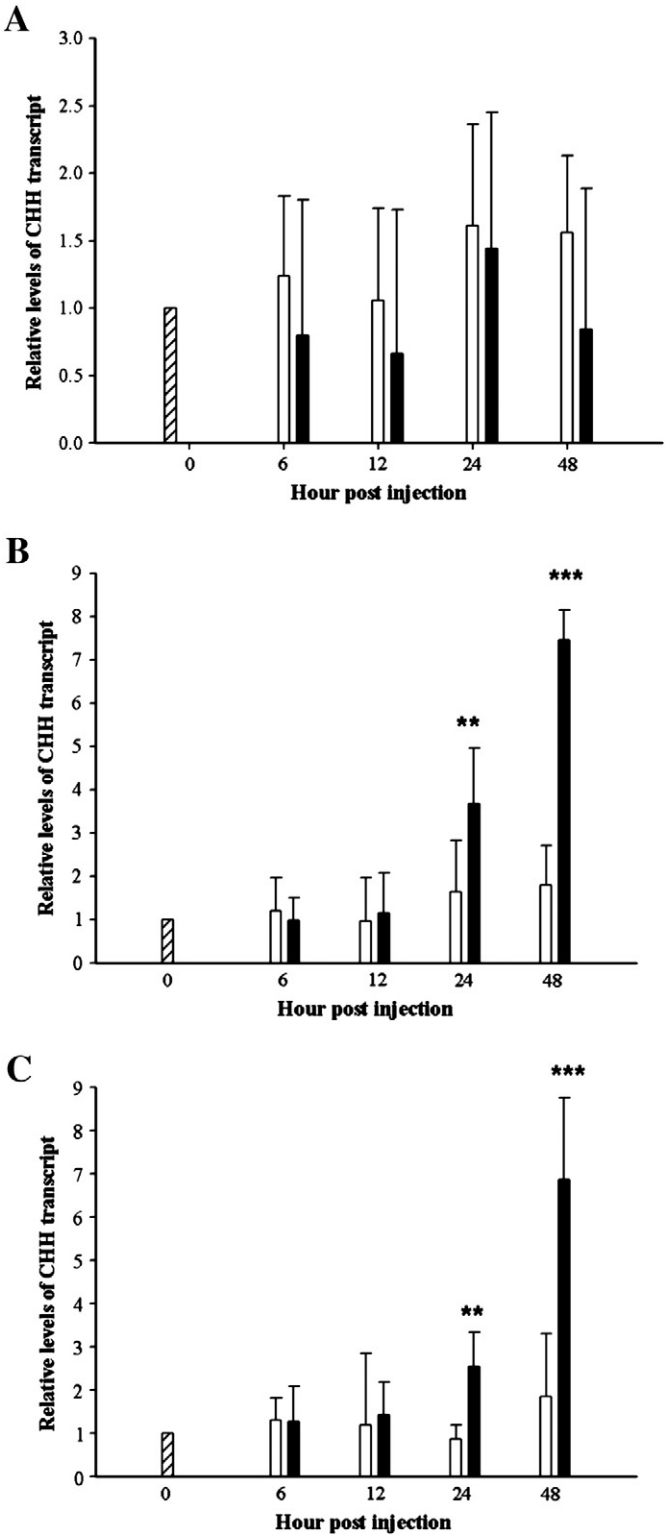

Fig. 5. Temporal profile of changes in the CHH transcript levels in the neuroendocrine tissues of white spot syndrome virus-infected and vehicle-treated crayfish. Animals were challenged with an injection of 0.01 M PBS (white bar) or PBS containing 2×10^6 viral particles (black bar). Tissues (A: the eyestalk ganglia; B: the thoracic ganglia; C: the cerebral ganglia) dissected from the animals before and at designated time points after injection was analyzed by a real-time polymerase chain reaction for quantification of CHH transcript. **, *** represent significant differences from the zero time values (hatched bar) at the levels of 0.01 and 0.005, respectively (n = 5 for each time point).

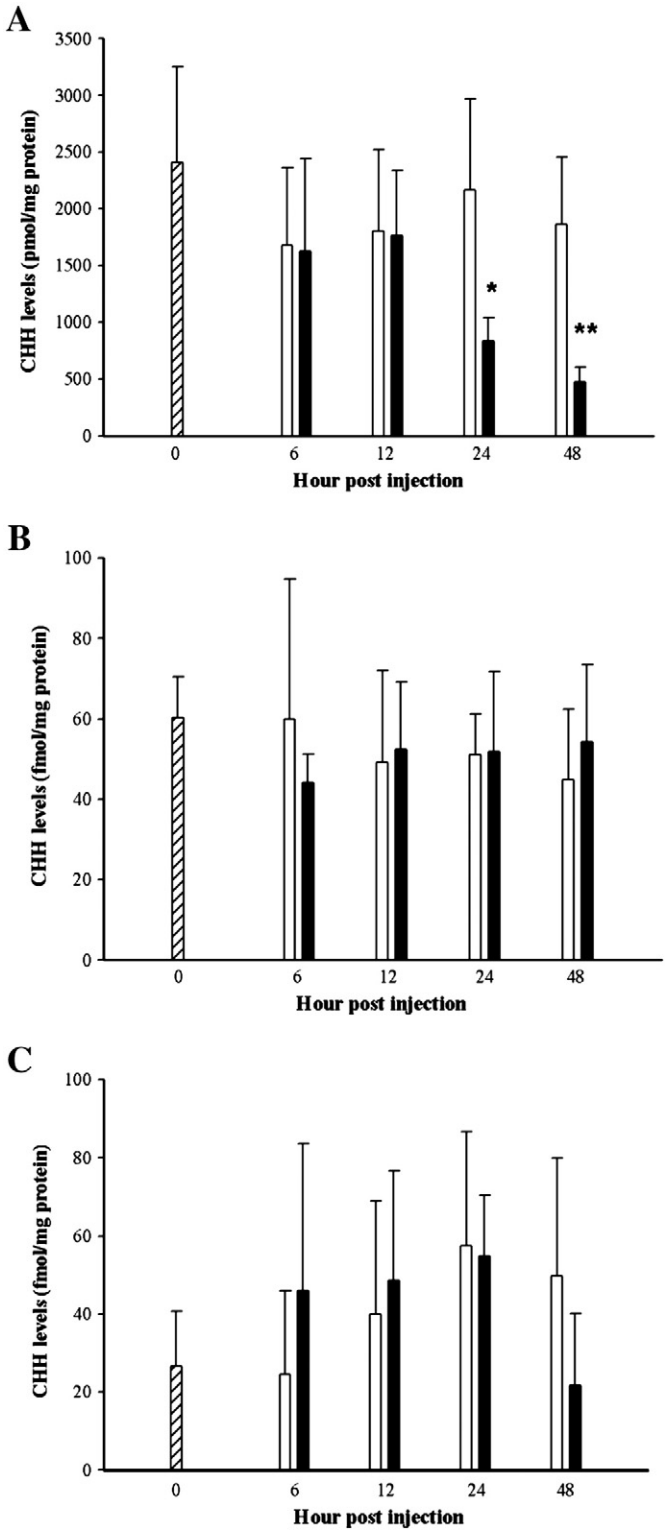

Fig. 6. Temporal profile of changes in the CHH peptide levels in the neuroendocrine tissues of white spot syndrome virus-infected and vehicle-treated crayfish. Animals were challenged with an injection of 0.01 M PBS (white bar) or PBS containing 2×10^6 viral particles (black bar). Tissues (A: the eyestalk ganglia; B: the thoracic ganglia; C: the cerebral ganglia) dissected from the animals before and at designated time points after injection was analyzed by a sandwich ELISA for quantification of CHH. *, ** represent significant differences from the zero time values (hatched bar) at the levels of 0.05 and 0.01, respectively (n = 5 for each time point).

activity of Glut1 is regulated by WSSV was not determined. Moreover, previous studies have shown that, in addition to its effect on glucose mobilization (see below), CHH also exerts a glycolysis-stimulating activity on its target tissues (Santos and Keller, 1993). Thus, it is likely that the WSSV-enhanced CHH release presented in the present study might mediate the stimulatory effect of virus on glycolytic activity in crustacean hosts.

In Norway lobsters (*Nephrops norvegicus*), the hemolymph glucose levels were significantly reduced after being infected with parasitic dinoflagellates (*Hematodinium* sp.), followed by a dramatic reduction in the glycogen contents in the hepatopancreas. It was suggested that the parasites act as a "carbohydrate sink", absorbing hemolymph glucose and hence forcing the hosts to mobilize glucose from carbohydrate-storage tissues such as the hepatopancreas to the extent that its glycogen contents were almost depleted in heavily infected animals (Stentiford et al., 2001). Like the parasitic dinoflagellates, WSSV would possibly avidly mobilize glucose from the carbohydrate-storage tissues through the glucose-mobilizing effect of CHH (see Santos and Keller, 1993). Whether this suggestion is valid or not it would require monitoring changes in tissue glycogen contents and hemolymph CHH levels over a longer period of time.

In summary, these data clearly demonstrated that WSSV activated the endocrine system of the host, specifically the expression and release of CHH. WSSV induced an increase in hemolymph CHH levels characterized by a rapid onset and a sustained duration. The WSSV-induced increase in hemolymph CHH levels primarily resulted from an enhanced release from the eyestalk ganglia, although the thoracic ganglia and cerebral ganglia are becoming more active in terms of CHH gene expression as the infection progresses. Further, it is suggested that the virus-enhanced CHH release would in effect act in favoring viral replication by modulating activity of carbohydrate metabolism, such as glucose mobilization and utilization. CHH-mediated changes in carbohydrate metabolism in virus-infected hosts, their implication for viral replication and host mortality, and the potential anti-WSSV applications are subjects worth studying.

Acknowledgments

The authors thank Prof. Chu-Fang Lo (Institute of Zoology, National Taiwan University) and the Core Facilities for Shrimp Functional Genomics for kindly providing the viral preparations. The present studies were supported financially by the National Science Council through a grant NSC98-2321-B-018-001-MY3 to C.-Y.L.

References

Abrantes, J.L., Alves, C.M., Costa, J., Almeida, F.C., Sola-Penna, M., Fontes, C.F., Souza, T.M., 2012. Herpes simplex type 1 activates glycolysis through engagement of the enzyme 6-phosphofructo-1-kinase (PFK-1). Biochim. Biophys. Acta 1822, 1198–1206.

Chang, E.S., Keller, R., Chang, S.A., 1998. Quantification of crustacean hyperglycemic hormone by ELISA in hemolymph of the lobster, *Homarus americanus*, following various stresses. Gen. Comp. Endocrinol. 111, 359–366.

Chang, E.S., Chang, S.A., Beltz, B.S., Kravitz, E.A., 1999. Crustacean hyperglycemic hormone in the lobster nervous system: localization and release from cells in the subesophageal ganglion and thoracic second roots. J. Comp. Neurol. 414, 50–56.

Chang, Y.-S., Liu, W.-J., Chou, T.-L., Lee, Y.-T., Lee, T.-L., Huang, W.-T., Kou, G.-H., Lo, C.-F., 2008. Characterization of white spot syndrome virus envelope protein VP51A and its interaction with viral tegument protein VP26. J. Virol. 82, 12555–12564.

Chang, Y.S., Chen, T.C., Liu, W.J., Hwang, J.S., Kou, G.H., Lo, C.F., 2011. Assessment of the roles of copepod *Apocyclops royi* and bivalve mollusk *Meretrix lusoria* in white spot syndrome virus transmission. Mar. Biotechnol. 13, 909–917.

Chen, S.H., Lin, C.Y., Kuo, C.M., 2005. *In silico* analysis of crustacean hyperglycemic hormone family. Mar. Biotechnol. 7, 193–206.

Chen, H.Y., Watson, R.D., Chen, J.C., Liu, H.F., Lee, C.Y., 2007. Molecular characterization and gene expression pattern of two putative molt-inhibiting hormones from *Litopenaeus vannamei*. Gen. Comp. Endocrinol. 151, 72–81.

Chen, I.T., Aoki, T., Huang, Y.T., Hirono, I., Chen, T.C., Huang, J.Y., Chang, G.D., Lo, C.F., Wang, H.C., 2011. White spot syndrome virus induces metabolic changes resembling the warburg effect in shrimp hemocytes in the early stage of infection. J. Virol. 85, 12919–12928.

Christie, A.E., 2008. Neuropeptide discovery in Ixodoidea: an *in silico* investigation using publicly accessible expressed sequence tags. Gen. Comp. Endocrinol. 157, 174–185.

Escobedo-Bonilla, C.M., Alday-Sanz, V., Wille, M., Sorgeloos, P., Pensaert, M.B., Nauwynck, H.J., 2008. A review on the morphology, molecular characterization, morphogenesis and pathogenesis of white spot syndrome virus. J. Fish. Dis. 31, 1–18.

Huang, H.T., Leu, J.H., Huang, P.Y., Chen, L.L., 2012. A putative cell surface receptor for white spot syndrome virus is a member of a transporter superfamily. PLoS One 7, e33216 http://dx.doi.org/10.1371/journal.pone.0033216.

Jiravanichpaisal, P., Sricharoen, S., Söderhäll, I., Söderhäll, K., 2006. White spot syndrome virus (WSSV) interaction with crayfish haemocytes. Fish Shellfish Immunol. 20, 718–727.

Kegel, G., Reichwein, B., Tensen, C.P., Keller, R., 1991. Amino acid sequence of crustacean hyperglycemic hormone (CHH) from the crayfish, *Orconectes limosus*: emergence of a novel neuropeptide family. Peptides 12, 909–913.

Keller, R., 1992. Crustacean neuropeptides: structures, functions, and comparative aspects. Experientia 48, 439–448.

Leu, J.H., Chang, C.C., Wu, J.L., Hsu, C.W., Hirono, I., Aoki, T., Juan, H.F., Lo, C.F., Kou, G.H., Huang, H.C., 2007. Comparative analysis of differentially expressed genes in normal and white spot syndrome virus infected *Penaeus monodon*. BMC Genomics 8, 120.

Leu, J.H., Yang, F., Zhang, X., Xu, X., Kou, G.H., Lo, C.F., 2009. Whispovirus. Curr. Top. Microbiol. Immunol. 328, 197–227.

Leu, J.H., Lin, S.J., Huang, J.Y., Chen, T.C., Lo, C.F., 2012. A model for apoptotic interaction between white spot syndrome virus and shrimp. Fish Shellfish Immunol. (http://dx.doi.org/10.1016/j.fsi.2012.05.030).

Livak, K.J., Schmittgen, T.D., 2001. Analysis of relative gene expression data using real-time quantitative PCR and the $2^{-\triangle\triangle Ct}$ method. Methods 25, 402–408.

Lo, C.-F., Hsu, H.-C., Tsai, M.-F., Ho, C.-H., Peng, S.-E., Kou, G.-H., Lightner, D.V., 1999. Specific genomic DNA fragments analysis of different geographical clinical samples of shrimp white spot syndrome virus. Dis. Aquat. Organ. 35, 175–185.

Lorenzon, S., Edomi, P., Giulianini, P.G., Mettulio, R., Ferrero, E.A., 2004. Variation of crustacean hyperglycemic hormone (cHH) level in the eyestalk and haemolymph of the shrimp *Palaemon elegans* following stress. J. Exp. Biol. 207, 4205–4213.

Montagné, N., Desdevises, Y., Soyez, D., Toullec, J.Y., 2010. Molecular evolution of the crustacean hyperglycemic hormone family in ecdysozoans. BMC Evol. Biol. 10, 62.

Morris, S., Postel, U., Mrinalini, Turner, L.M., Palmer, J., Webster, S.G., 2010. The adaptive significance of crustacean hyperglycaemic hormone (CHH) in daily and seasonal migratory activities of the Christmas Island red crab *Gecarcoidea natalis*. J. Exp. Biol. 213, 3062–3073.

Noch, E., Khalili, K., 2012. Oncogenic viruses and tumor glucose metabolism: like kids in a candy store. Mol. Cancer Ther. 11, 14–23.

Rodríguez, J., Ruiz, J., Maldonado, M., Echeverría, F., 2012. Immunodetection of hemocytes, peneidins and $\alpha(2)$-macroglobulin in the lymphoid organ of white spot syndrome virus infected shrimp. Microbiol. Immunol. 56, 562–571.

Sánchez-Paz, A., 2010. White spot syndrome virus: an overview on an emergent concern. Vet. Res. 41, 43.

Santos, E.A., Keller, R., 1993. Crustacean hyperglycemic hormone (CHH) and the regulation of carbohydrate metabolism: current perspectives. Comp. Biochem. Physiol. A 106, 405–411.

Silva da Costa, L., Pereira da Silva, A.P., Da Poian, A.T., El-Bacha, T., 2012. Mitochondrial bioenergetic alterations in mouse neuroblastoma cells infected with Sindbis virus: implications to viral replication and neuronal death. PLoS One 7, e33871 http://dx.doi.org/10.1371/journal.pone.0033871.

Soyez, D., 1997. Occurrence and diversity of neuropeptides from the crustacean hyperglycemic hormone family in arthropods. Ann. N. Y. Acad. Sci. 814, 319–323.

Stentiford, G.D., Chang, E.S., Chang, S.A., Neil, D.M., 2001. Carbohydrate dynamics and the crustacean hyperglycemic hormone (CHH): effects of parasitic infection in Norway lobsters (*Nephrops norvegicus*). Gen. Comp. Endocrinol. 121, 13–22.

Tsai, K.-W., Chang, S.-G., Wu, H.-J., Shih, H.-Y., Chen, C.-H., Lee, C.-Y., 2008. Molecular cloning and differential expression pattern of two structural variants of the crustacean hyperglycemic hormone family from the mud crab *Scylla olivacea*. Gen. Comp. Endocrinol. 159, 16–25.

Wang, C.-H., Lo, C.-F., Leu, J.-H., Chou, C.-M., Yeh, P.-Y., Chou, H.-Y., Tung, M.-C., Chang, C.-F., Su, M.-S., Kou, G.-H., 1995. Purification and genomic analysis of baculovirus associated with white spot syndrome (WSBV) of *Penaeus monodon*. Dis. Aquat. Organ. 23, 239–242.

Wang, H.C., Wang, H.C., Leu, J.H., Kou, G.H., Wang, A.H., Lo, C.F., 2007. Protein expression profiling of the shrimp cellular response to white spot syndrome virus infection. Dev. Comp. Immunol. 31, 672–686.

Webster, S.G., 1996. Measurement of crustacean hyperglycemic hormone levels in the edible crab *Cancer pagurus* during emersion stress. J. Exp. Biol. 199, 1579–1585.

Webster, S.G., Keller, R., Dircksen, H., 2012. The CHH-superfamily of multifunctional peptide hormones controlling crustacean metabolism, osmoregulation, moulting, and reproduction. Gen. Comp. Endocrinol. 175, 217–233.

Wu, H.J., Tsai, W.S., Huang, S.Y., Chen, Y.J., Chen, Y.H., Hsieh, Y.R., Lee, C.Y., 2012a. Identification of crustacean hyperglycemic hormone (CHH) and CHH-like (CHH-L) peptides in the crayfish *Procambarus clarkii* and localization of functionally important regions of CHH. Zool. Stud. 51, 288–297.

Wu, S.H., Chen, Y.J., Huang, S.Y., Tsai, W.S., Wu, H.J., Hsu, T.T., Lee, C.Y., 2012b. Demonstration of expression of a neuropeptide-encoding gene in crustacean hemocytes. Comp. Biochem. Physiol. A 161, 463–468.

Yeh, F.C., Wu, S.H., Lai, C.Y., Lee, C.Y., 2006. Demonstration of nitric oxide synthase activity in crustacean hemocytes and anti-microbial activity of hemocyte-derived nitric oxide. Comp. Biochem. Physiol. B 144, 11–17.

Yu, Y., Clippinger, A.J., Alwine, J.C., 2011. Viral effects on metabolism: changes in glucose and glutamine utilization during human cytomegalovirus infection. Trends Microbiol. 19, 360–367.

Zou, H.S., Juan, C.C., Chen, S.C., Wang, H.Y., Lee, C.Y., 2003. Dopaminergic regulation of crustacean hyperglycemic hormone and glucose levels in the hemolymph of the crayfish *Procambarus clarkii*. J. Exp. Zool. 298, 44–52.